

Using pattern homogenization of binary grayscale masks to fabricate microfluidic structures with 3D topography†

Javier Atencia,^a Susan Barnes,^b Jack Douglas,^b Mark Meacham^a and Laurie E. Locascio^{*a}

Received 20th June 2007, Accepted 28th August 2007

First published as an Advance Article on the web 31st August 2007

DOI: 10.1039/b709369a

Because fluids at the microscale form three dimensional interfaces and are subject to three dimensional forces, the ability to create microstructures with modulated topography over large areas could greatly improve control over microfluidic phenomena (*e.g.*, capillarity and mass transport) and enable exciting novel microfluidic applications. Here, we report a method for the fabrication of three-dimensional relief microstructures, based on the emergence of smooth features when a photopolymer is exposed to UV light through a transparency mask with binary motifs. We show that homogeneous features emerge under certain critical conditions that are also common to other, apparently unrelated, phenomena such as the emergence of macroscopic continuum properties of composite materials and the rates of ligand binding to cell membrane receptors. This fabrication method is simple and inexpensive, and yet it allows for the fabrication of microstructures over large areas (centimetres) with topographic modulation of features with characteristic dimensions smaller than 100 micrometres.

Introduction

Microfluidic systems are widely used across many fields such as analytical chemistry,¹ single molecule detection² and biological cell studies,³ and in many applications that take advantage of the unique physical properties of microscale interfaces.⁴ Planar lithography, the most common fabrication technology used in microfluidics, has been optimized for microelectronics, a binary world where it is critical to create high resolution two-dimensional (2D) patterns with vertical sidewalls (“all-or-none” patterning). This invariably results in flat topographies; however, the ability to contour microscale topography in three dimensions (3D) is crucial for the microscale manipulation of liquids, which are inherently subject to 3D forces and form 3D interfaces. Although it is possible to generate multilevel features using planar lithography, the approach is time consuming (mask alignment and UV exposure needs to be repeated for each level), and the method does not allow generation of smooth transitions between levels.

There are several technologies that can be used to create 3D topographies on a photoresist, such as e-beam lithography⁵ and two-photon lithography⁶ among others.^{7–10} However these methods require special equipment, and in some cases, are time consuming for the fabrication of microfluidic devices where a compromise in feature resolution is often acceptable,¹¹ but the ability to pattern large areas (centimetres) is usually a must.

Of special interest are the “grayscale technologies” where a photoresist is exposed to UV light through a mask that can be

designed with several levels of light transmission. These masks can be continuous¹² (with excellent resolution and high cost), or discrete. In the last case (conventional grayscale lithography for MEMs), a mask having transparent and opaque pixels is used to expose a conventional photoresist to UV light.¹³ The mask pixels are designed to have size and pitch (distance between pixels) below the optical resolution of the system (minimum feature that can be resolved), thereby, producing a smoothing effect. Different levels of light transmission are achieved by increasing or decreasing the size of a pixel within its pitch. This method has been shown to be extremely useful for MEMs fabrication, but it is still costly (requires expensive chrome masks) and is *de facto* not practical for patterning large areas because of the amount of data needed to define all of the pixels (area scales linearly with number of pixels squared). An alternative to chrome masks for grayscale lithography is to use inexpensive transparency masks and reduce the designs using an array of micro lenses.¹⁴ Although this approach is cost-effective, it is only valid for features of $\approx 100 \mu\text{m}$ in diameter and can only generate arrays of repetitive features.

Several fabrication technologies have been recently proposed for microfluidic fabrication due to the inadequacy of conventional grayscale technology to pattern large areas. These methods, which can be considered unconventional grayscale techniques, include (1) using microfluidic photomasks,¹⁵ (2) overexposure of a photoresist to create non-linear polymerization¹⁶ and (3) using colored masks to block UV light.¹⁷

In the first case, a PDMS layer with microchannels is placed directly in contact with the photoresist that is going to be exposed to UV light. Dyes with different concentrations are flowed through the channels. Light transmission is a function of the dye concentration that is flowing through the channel at that particular moment. Since the flow is laminar, one can introduce gradients of different concentrations in a

^aBiochemical Science Division, NIST, Gaithersburg, USA.
E-mail: laurie.locascio@nist.gov; Tel: +1 (301) 975-3130

^bPolymers Division, NIST, Gaithersburg, USA

† Electronic supplementary information (ESI) available: Figure S1–Determination of homogeneous/discrete patterns for the optical adhesive Norland R-81; and Figure S2–Fabrication of ejector plate with an array of horns. See DOI: 10.1039/b709369a

microchannel to produce smooth topographic gradients on the photoresist. The main limitation of this approach is that it does not allow for the creation of structures with arbitrary height in the two directions of the plane simultaneously; *i.e.*, it is possible to maintain a gradient of concentration across a channel, but not along the channel.

In the second case, the method exploits the non-linear polymerization of SU8 that occurs due to diffraction when a small opaque region within a transparent region of the mask is overexposed to UV light. Though this technique can be used to create posts or small structures of different heights inside a microchannel, it can not be used to modulate the topography of an entire microchannel.

In the third case, the mask is generated with a high definition color printer. Different inks have different UV absorption characteristics, thus, it is possible to print different color mixtures and obtain multilevel structures on the photoresist. Although it is a very simple and promising technique, its main drawback is the low resolution of the structures that it can generate.

Here, we present a method for the fabrication of polymeric masters with microstructures of modulated topography using binary grayscale masks. This method differs conceptually from conventional grayscale technology in that it utilizes a low contrast photoresist (an optical adhesive) and a homogenization effect based on diffraction and non-linear polymerization. With this method, the mask pixels can be significantly larger than the optical resolution of the system, which is key to patterning large areas with inexpensive transparency masks and conventional photolithographic equipment. Other properties of this technique are (i) ease of design; (ii) fast turn-around times both for mask design and fabrication (virtually just the exposure times); (iii) low cost; and yet (iv) it allows patterning of large areas with topographic resolution of decades of microns. We show the feasibility and simplicity of the approach with several examples.

Homogenization transition

We use ‘homogenization transition’ to refer to the discrete particle-to-continuum transition that occurs, for example, when macroscopic continuum properties of different materials (*e.g.*, viscosity, friction and conductivity) emerge from the interaction of collections of atoms, molecules and particulate species, and from filler particles dispersed in a matrix with different material properties (*i.e.*, composites). In many problems of this kind, this transition is sharp and is not dictated by the particle density, but by the overlapping of non-linear fields generated by each particle. In the ‘‘homogeneous state’’, the particles lose their identity, and the whole structure becomes insensitive to fluctuations in particle concentration.

The homogenization transition also appears in other diverse contexts, such as the light scattering due to water droplets that are invisible when dispersed in the atmosphere but appear as ‘‘solid’’ when they cluster to form clouds,¹⁸ and many diffusion-controlled phenomena, which include the friction coefficient f of complex Brownian particles,¹⁹ the rates of diffusion-limited reactions in catalysis, the rates of cooling and

heating by complex shaped objects²⁰ and the rates of ligand binding to cell membrane receptors.²¹ In the last case, for instance, the membrane of a cell does not need to be fully covered by receptors to optimally detect ligands. Instead, beyond a (typically low) critical concentration of receptors, which is a function of the product na , where n is the number of receptors, and a is a functional describing the receptor shape (*e.g.*, the radius for a disk), the addition of new receptors does not improve substantially the detection capability of the membrane, and thus, the membrane effectively behaves as if it were fully covered by receptors.²¹

In the fabrication method presented here (which we term grayscale fabrication using pattern homogenization or GFPH) an optical adhesive is exposed to UV light through a transparency mask (Fig. 1a) with binary patterns made of transparent and opaque pixels. Here we show that, intriguingly, the transition where binary motifs in the mask are transferred as homogeneous surfaces (where the pixel geometry is not apparent) is not dictated by the ratio or transparent area to total area in a given region of the mask, (*i.e.*, na^2 , where n is the number of transparent pixels per unit area and a the side length of a square pixel) but by the number of transparent pixels and their individual diameter (na), which contradicts intuition, and follows the law for homogenization transition stated above. We utilize the emergence of this homogenization effect to fabricate microstructures with smooth surfaces and modulated topography in a single photolithographic step.

Results and discussion

Our general approach utilizes a high resolution transparency ink mask (3000 dpi film output) with grayscale patterns made of binary opaque/transparent pixels, an optical adhesive that we use as photoresist,²² conventional photolithography

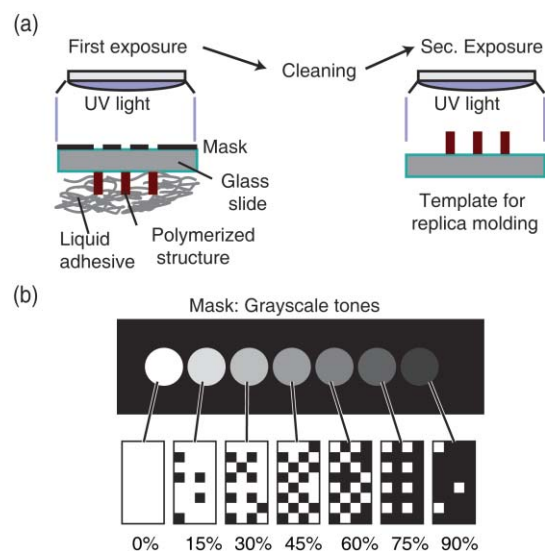


Fig. 1 Grayscale fabrication with pattern homogenization. (a) A glass slide is brought into contact with the optical adhesive, and a mask with grayscale patterns (made of transparent and opaque pixels) is used to selectively block UV light. (b) Example of grayscale tone masks and corresponding binary tiling units or ‘‘swatches’’ (in this case made of 8×4 pixels).

equipment (e.g., collimated UV light source) and a graphics software program to design the masks. Briefly, a clean glass slide in contact with the optical adhesive is exposed to UV light through the grayscale mask (Fig. 1a, see also Experimental). UV light triggers a polymerization front that propagates in the direction perpendicular to the glass surface, with a velocity that is a function of the transmitted intensity of the light.^{22,23} Subsequently, the unpolymerized material is removed and the remaining structures are again exposed to UV light for full polymerization. The glass slide with the final structures is used as a master to create a polymer replica (e.g. PDMS)²⁴ that is bonded to a glass slide to form the final microfluidic devices.

Homogenization transition: transfer of binary motifs from a mask as homogeneous surfaces on a photopolymer

We use an optical adhesive with low contrast $\gamma \approx 0.55$ as photoresist²⁵ (the contrast is a measure of the ability of a resist to distinguish between transparent and opaque areas of a mask)²⁶ to promote partial polymerization in areas subject to diffracted light. Specifically, under an opaque pixel there is an overlapping of the exponential decay in light intensity from each edge (due to diffraction)¹⁶ that, in addition to the non-linear nature of photopolymerization, can produce partial polymerization between features and eventually result in the emergence of homogeneous surfaces with topographical height determined by the total dose of UV light.

For simplicity, we created a library of tiling pattern units (“swatches”; Fig. 1b), that we use as repetitive motifs to define areas with the same light transmittance. Each swatch is a distinct array of pixels where the relative density of transparent to opaque pixels determines the average intensity of the transmitted UV light.

A simple experiment was carried out to explore the emergence of the homogenization phenomenon with different masking patterns. We designed a transparency mask with a set of circular areas, each tiled with a different 8×4 swatch (swatch formed by 8×4 pixels; Fig. 1b), that differ in either average “grayscale tone” (the ratio of transparent to opaque pixels where 0% is completely transparent and 100% completely opaque) or in pixel size. The mask was used to fabricate an array of polymerized structures (see ESI, Fig. S1)† that we employed to determine first, whether it is possible to create homogeneous features with binary masking patterns, and second, under what conditions the emergence of homogeneous patterns occurs.

Fig. 2a is an example of the determination of the homogenization transition for a given grayscale tone (e.g., 75%) and decreasing pixel size. In this example, below a pixel size value ($42 \mu\text{m}$) the masking motif is transferred as a flat surface, and above a different pixel size value ($127 \mu\text{m}$) the pixels in the masking motif are transferred as individual posts to the photoresist. We found that there is a homogenization transition for every grayscale tone where binary patterns on the mask are transferred to the photoresist as homogeneous polymerized patterns, Fig. 2b (\square), or discrete polymerized patterns where the pixel geometry is apparent (one post per pixel), Fig. 2b (\blacktriangle). Interestingly, this transition does not depend just on the pixel density or the total area of transparent

pixels, but instead is found to occur for a critical value of the product na , where n is the number of transparent pixels per unit area, and a is the side length of the pixel (and, counterintuitively, not its area), as in the classical receptor problem described previously. Specifically, we found that if $na > 5500 \mu\text{m}$ per unit of patterned area (in mm^2), the pattern is transferred as a homogeneous smooth surface, and if $na < 3000 \mu\text{m mm}^{-2}$, it is transferred as a collection of pixelated patterns (Fig. 2c). This critical concentration for homogenization can then be exploited to create discrete and smooth functional photopolymerized features as required in a particular application.

The grayscale homogenization transition depends on the polymerization characteristics of the photoresist, and thus it is different to the principle used in conventional binary grayscale technologies (maintaining pixel size and pixel pitch below the optical resolution of the photolithographic system).¹³ With the method here described, patterns of different pixel size can be used simultaneously to create smooth surfaces (and thus optimize the amount of data needed to define the patterns), as far as the grayscale transition inequality is satisfied. Additionally, it is also possible to use large pixels to generate smooth multilevel surfaces (and fill large areas), and simultaneously use small pixels to create small vertical posts (see Fig. 2B). The homogenization transition is not function of the pixel size but of the product na .

The relation between grayscale tone and polymerized feature height is reproducible, but complex to predict; it requires an accurate knowledge of the light intensity at the surface of the optical adhesive,^{22,23} and the transmittance of light through grayscale patterns becomes increasingly non-linear as the pattern pixel size approaches the printing resolution of the mask. In the present work, we utilize a simple calibration method to empirically determine this relation for a set of swatches that produce homogeneous features and design microfluidic systems *a posteriori*. For example, Fig. 3a shows calibration curves obtained empirically for the relation between grayscale tone (made of 8×4 swatches) and feature height for masks with the same motifs and different pixel sizes, 2400 ppi and 600 ppi.²⁷ Each swatch produces a specific photopolymerized structure of a distinct height, and therefore, we can use them as building blocks in a hierarchical design approach for the creation of complex polymerized patterns.

Microfluidic structures with 3D topography: design and fabrication of microfluidic templates

Multilevel flat structures can be easily fabricated by designing adjacent large areas with swatches of different grayscale tones using calibration curves (Fig. 3a). We measured a sidewall angle of $\approx 85^\circ$ for medium to low grayscale tones.²⁸ Fig. 3c shows a multilevel microchannel network with varying widths and heights made with a single transparency mask and UV exposure. Multilevel structures fabricated in a single step would greatly facilitate applications taking advantage of capillary forces in priming flows, applications where microchannels are coupled to larger wells or cavities, e.g., to contain microfluidic pumps,²⁹ or high-throughput screening applications with a large number of microchannels, inlets and outlets.³⁰

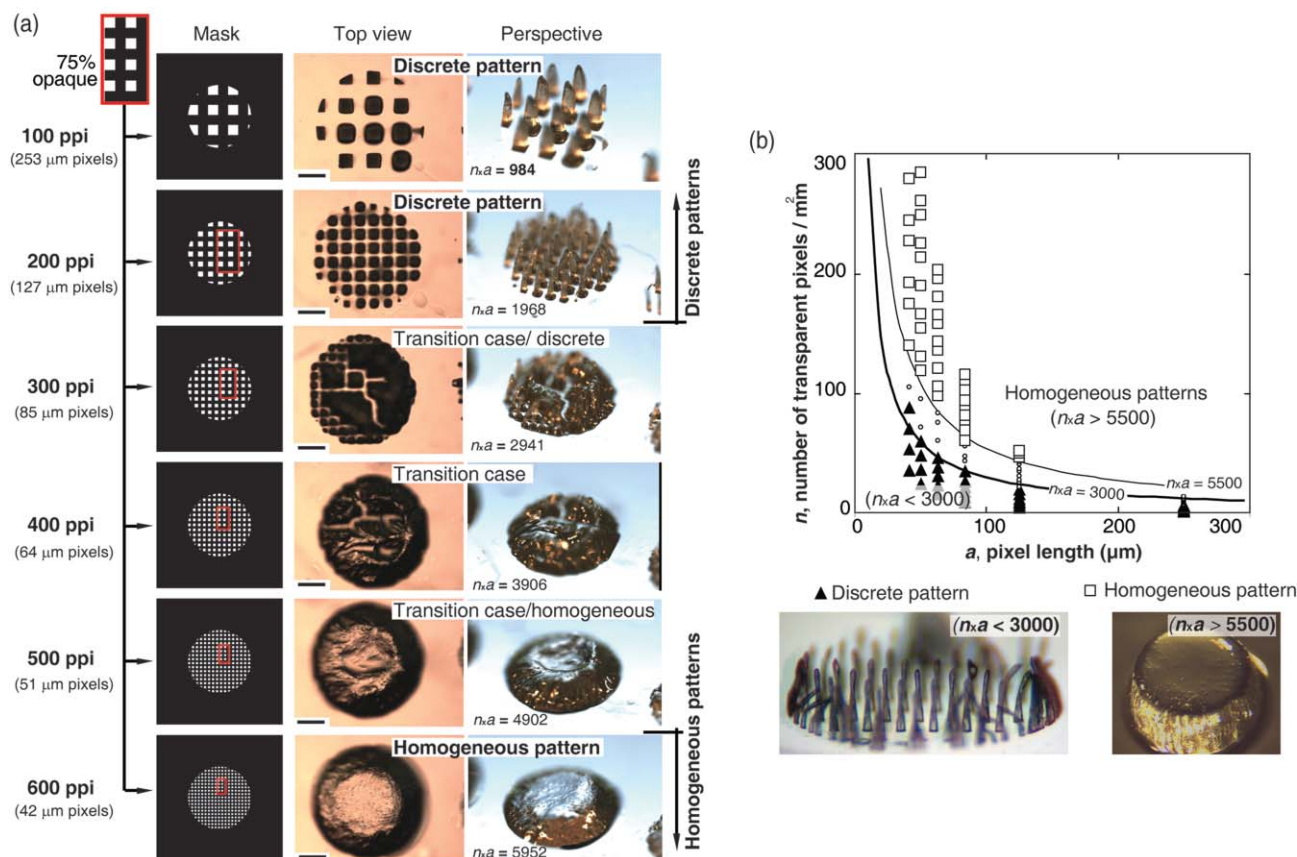


Fig. 2 Homogenization transition. There is a transition where binary masking motifs are transferred to a photopolymer either as discrete or homogeneous patterns. The transition occurs as a function of the number of transparent pixels per area (thus, the grayscale tone), and the pixel size. (a) Example of the determination of the homogenization transition with an 8×4 swatch of 75% grayscale value and different pixel sizes. (b) Diagram showing the morphology transition in an array of 8×4 swatches of different pixel size and density of transparent pixels. The photopolymerized features corresponding to this diagram are displayed in the ESI, Fig. S1.† The adhesive polymerizes forming individual posts (\blacktriangle) if $na < 3000$, where n is the number of transparent pixels per unit area of the patterned mask and a the side length of a pixel, and it polymerizes forming homogeneous macro surfaces (\square) if $na > 5500$. The symbol (\circ) denotes transition cases between homogeneous and discrete patterns. Scale bars are $400 \mu\text{m}$.

Curved surfaces can also be created with GFPH by designing incremental grayscale tones in adjacent small areas. After the first exposure to UV light, the polymer at the surface is in a compliant gel-like state that can stick to itself during cleaning, thereby smoothing the transitions between surfaces of similar heights. We have generated semicircular microchannels by using swatches of 5×1 pixels that we enlarged with graphic-design software to form lines (Fig. 4a). The complexity of the curved surfaces can be increased with simple graphic operations such as stretching, rotating and skewing. For example, we used a second pattern of lines to generate a microchannel of smaller diameter, skewed the patterns 30 degrees and then overlaid the second pattern on top of the first to obtain a semi-circular microchannel with a semi-spiral ridge inside (Fig. 4b,c). In yet another illustration, we combined 8×4 pixel swatches for multilevel flat surfaces with 5×1 swatches to produce a microchannel with a zigzag structure that is modulated in the three x , y and z directions (Fig. 4d). We stress that fabrication of the latter patterns cannot be performed with either conventional lithography or microfluidic photomasks.¹⁵ These complex geometries can be useful for many applications, such as to create tailored 3D

flow patterns inside the microchannel to promote chaotic advection,^{31–33} to create arbitrary cross sections in the microchannel that yield in plane velocity profiles different from Poiseuille flow for pressure driven systems or to modify the cross sectional distribution of the electric field in electroosmotic flow to eliminate electric field constriction.

We use swatches with different hierarchical levels to design complex microfluidic devices. Typically, the first level defines the grayscale tones for simple geometries such as the ones considered in the previous examples, and higher levels increase the degree of complexity. As an illustration of the possibilities of this approach, we fabricated an array of polymerized “horns” that we used as a master for a microfluidic ejector of monodisperse liquid droplets into air. First, we designed a single horn with concentric circles patterned with different tonalities of first-level grayscale 8×4 swatches, that varied monotonically from black in the outer circle (1 mm outer diameter) to white in the inner circle ($50 \mu\text{m}$ diameter), as shown in Fig. 5a. This design was used to define a second-level swatch, and apply it to pattern a large rectangle with the same repetitive motif (Fig. 5b). First-level swatches used to generate multilevel microchannels or other curved surfaces can be easily

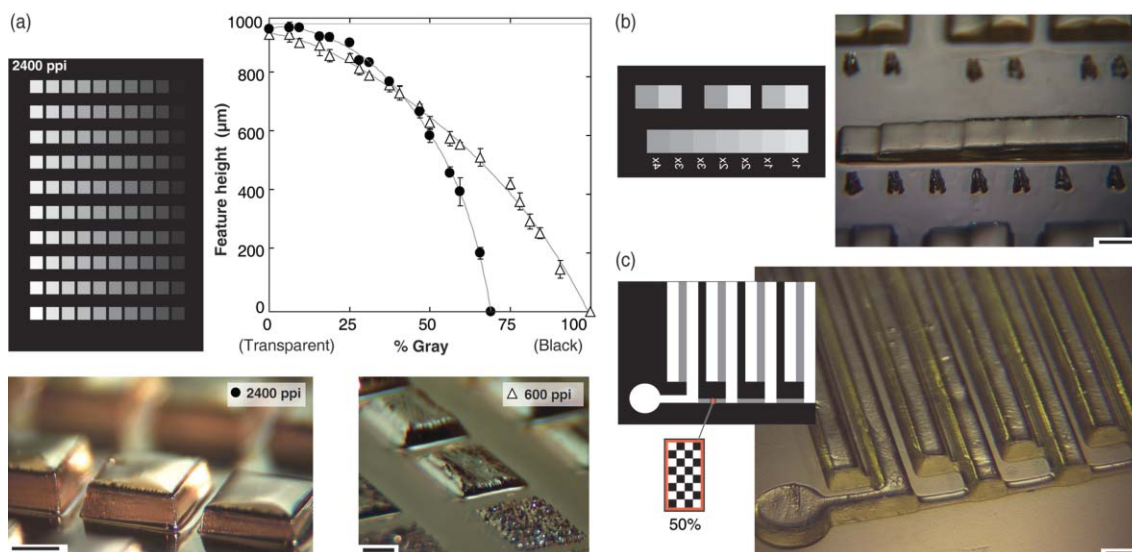


Fig. 3 Homogeneous multilevel flat surfaces. (a) Calibration experiments to find the relation between grayscale tone and feature height for two pixelation grades. On the top left, grayscale mask at 2400 dpi and 3000 dpi²⁷ utilized to generate a curve (●). The same calibration experiment was repeated with a mask at 600 dpi and 3000 dpi (○). The curves differ due to the error introduced as the pixelation resolution approaches the printing resolution. Scale bars are 1 mm. (b) Multilevel stepped channels can be fabricated by designing large adjacent areas with grayscale values calibrated in (a). Scale bar is 2 mm. (c) Example of a device with microchannels of different widths and heights fabricated using a single mask. Scale bar is 2 mm.

added to the design. The thiolene master was then used to cast a thiolene replica that was mounted over a PDMS gasket and piezoelectric actuator to form a sandwich structure around a fluid cavity (Fig. 5c; see also Experimental and ESI Fig. S2).† Operated at a specific frequency, the piezoelectric transducer produces standing acoustic waves that are focused by geometrical reflections within the horns, creating a pressure gradient that can be used for fluid jet ejection.³⁴ We used the microfluidic device to eject water through the thiolene nozzle orifices at 5 ml min⁻¹ flow rate (Fig. 5c). The diameter of the nozzle orifices (≈40 μm) is well suited to cell manipulation *via* focused mechanical forces to enable various biophysical effects such as the uptake of small molecules or gene delivery and transfection,³⁵ additionally, the grayscale mask could be designed to create nozzle orifices of different sizes for application to areas as diverse as mass spectrometry, fuel processing, manufacture of multilayer parts and circuits, and deposition of photoresist without spinning. Our fabrication approach confers a degree of flexibility on the design of the horn geometry that is not possible to achieve by conventional methods (*e.g.*, anisotropic wet etching of a silicon wafer).³⁴

Conclusions

GFPH differs from conventional binary grayscale fabrication technology¹³ in its principle (homogenization transition) and its form (hierarchical design approach). Both features are key to make this technique overcome the limitations of conventional grayscale technology for patterning large areas, and in particular for microfluidic applications. Additionally, the technique is simple, inexpensive and uniquely suited for patterning large areas with 3D relief structures within a range of dimensional sizes and resolution.³⁶ We believe that the

ability to fabricate microfluidic devices with 3D topography will promote the emergence of new microfluidic functionalities. Further, the use of photopolymerizable materials with different viscosity, contrast and polymerization resolution should allow for the fabrication of microfluidic channels and other microstructures within smaller size ranges.

Experimental

Fabrication protocol

Grayscale binary masks were designed with Adobe Illustrator and printed at 3000 dpi (dots per inch; we use “pixels per inch” or “ppi” to refer to pixelation resolution) and low density by Media Fusion (<http://mfiprepress.com>). Glass slides 75 × 50 × 1 mm (Corning) were used as substrates for the thiolene masters. The glass slides were exposed to UV–ozone with an ultraviolet ozone cleaning system T10X10/OES (UVOCS) for 20 min and placed in conformal contact with a polydimethylsiloxane (PDMS) gasket containing the thiolene-based liquid adhesive (R-81 Norland). The transparency mask was stacked between the other side of the glass slide and a second glass slide, with a thin layer of DI water in between mask and slides. UV exposure was performed with collimated light from a MA8 mask aligner (Suss) or with an Omnicure Series 2000 (Exfo). Typical doses ranged from 15 mW cm⁻² for 8 s to 1.5 μW cm⁻² for 500–900 s. After pre-cure the un-crosslinked material was removed by first blowing with clean air followed by a three step rinse with IPA (isopropyl alcohol), acetone and again IPA to remove the acetone. The cleaning step is critical, since too much pressure of air and long exposure to acetone can bend or destroy patterns. We used post-cure UV energy doses of ≈12 J. PDMS replicas were fabricated *via* the usual replica molding techniques.²⁴ Holes in the PDMS replicas were

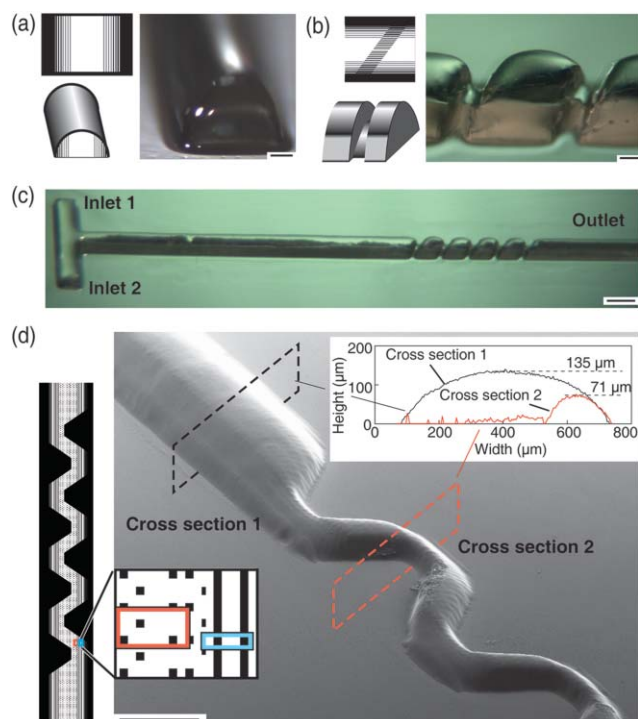


Fig. 4 Curved surfaces generated with a single transparency mask. (a) The mask was created with first-level 5×1 swatches (arrays of 5×1 transparent and opaque pixels), that were elongated along the length of the microchannel to form lines. Two axis symmetric grayscale gradients define the curved sides of the microchannel. Scale bar is $200 \mu\text{m}$. (b) The same type of swatches was used to create a microchannel of smaller diameter that was skewed and overlaid on top of the patterns of the previous panel, rendering a single semi-spiral ridge. Scale bar is $200 \mu\text{m}$. (c) The patterns in the previous panel were repeated several times along the main channel to build a “T” channel with a semi-screw mixer with a single mask. Scale bar is 1 mm . (d) Simultaneous modulation in the x , y and z directions of the mixing part in a “T” channel. On the left, detail of an 8×4 swatch (10%) and a 5×1 swatch (60%) used to pattern the master. Scale bar is $200 \mu\text{m}$.

punched with blunt syringe needles 21 G NE-211PL (Small Parts) or metal tubing HTX-27T (Small Parts).

Jet ejector

To fabricate the thiolene horn array replicas (see ESI, Fig. S2)† we used hydrophobic thiolene masters (the master was sputtered with layers of chrome ($\approx 10 \text{ nm}$) and gold ($\approx 100 \text{ nm}$), and exposed to heptadecafluoro-1,1,1,2,2-tetrahydrodecyl trichlorosilane (Gelest) in a vacuum container for 12 h). The thiolene-based liquid adhesive was poured over the master, and a thin PDMS membrane supported by a glass slide was used to top the master and the liquid adhesive. The horns of the thiolene master were pressed into the PDMS and after photopolymerization the thiolene replica was peeled off. The liquid jet ejector comprising the horn array, PDMS gasket and piezoelectric transducer, Fig. 5(c), was assembled between pieces of polycarbonate and aluminum as shown in the ESI Fig. S2.† A function generator (Stanford Research Systems DS345) and a linear RF amplifier (T&C Power Conversion AG1020) were used to operate the jet ejector.

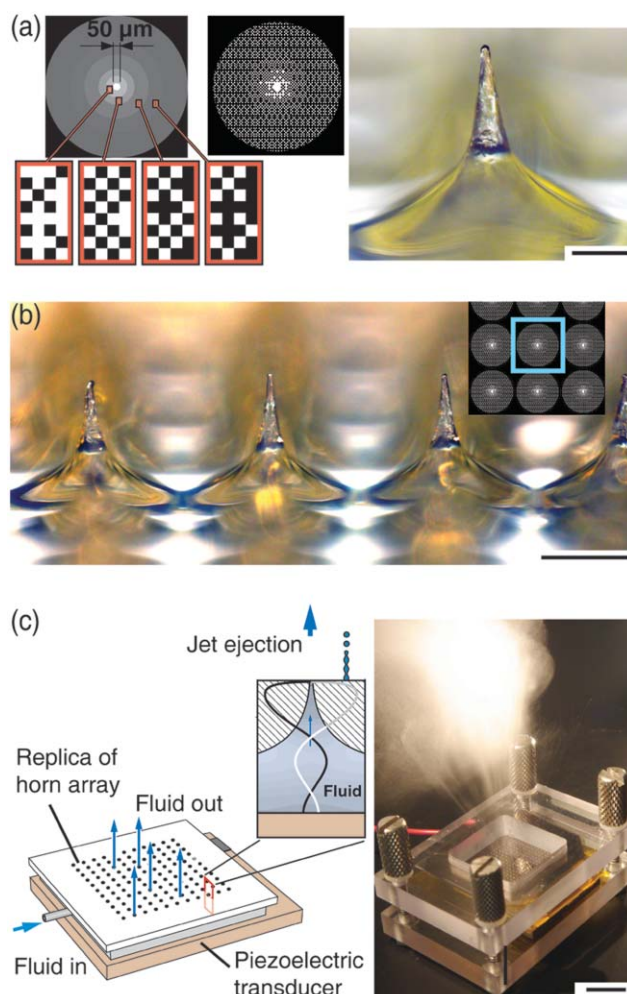


Fig. 5 Hierarchical patterning of complex structures over large areas. (a) On the left, a compound of concentric circles of different grayscale tones is designed for the fabrication of a single “horn”. The 8×4 swatches from left to right correspond to a 35%, 45%, 60% and 65% grayscale tone. In the centre, the design is pixelated using first-level 8×4 swatches. On the right a thiolene “horn” created with the previous mask. Scale bar is $200 \mu\text{m}$. (b) The design of a single horn on the previous panel was used as a second-level switch to pattern an array of horns over a large rectangular area ($20 \times 20 \text{ mm}^2$). The mask was used to fabricate a template of a master array of thiolene horns that was replicated as a hard membrane with arrayed cavities (ESI Fig. S2).† Scale bar is $500 \mu\text{m}$. (c) On the left, schematic illustrating the operation of an ultrasonic atomizer. A piezoelectric transducer produces pressure waves that are focused by the geometry of the cavities in the membrane, leading to ejection of jets of liquid (shown on the right side). Scale bar is 1 cm .

Imaging

Photographs were either taken with a Coolpix 8800 VR camera (Nikon) or a PL-A623C camera (Pixelink) that was mounted on one of two stereoscopes (LW Scientific IS-2Z or Olympus MVX10). Scanning electron microscope (SEM) images were taken with an Ultra-60 FESEM (Zeiss) after sputtering layers of chrome ($\approx 10 \text{ nm}$) and gold ($\approx 100 \text{ nm}$) over the thiolene masters.

Topography characterization

To measure the height of the posts in Fig. 2(a) we fabricated a thiolene master with 100 posts (from 1% to 100% grayscale) and cut the glass slide into strips containing single rows of posts. We took photographs perpendicular to the plane of the cut of every strip and measured the height of the posts directly from the photographs using Adobe Illustrator. We extracted a single value for the height of each post by averaging the height across the whole surface. To determine the topography of the curved structures in Fig. 4(d), we created a PDMS replica of the master, bonded it to a glass slide to form a microchannel, and introduced a solution of Fluorescein (Molecular Probes) in water (50 molar) using an external syringe pump (Harvard Apparatus PHD 2000) at a constant flow rate of 0.2 ml min^{-1} . We visualized the flow with a confocal microscope LSM 510 Meta (Zeiss), processed the data and obtained the topographic height using the LSM 510 Meta (Zeiss) software.

Disclaimer

Certain commercial equipment, instruments or materials are identified in this report to specify adequately the experimental procedure. Such identification does not imply recommendation or endorsement by the National Institute of Standards and Technology, nor does it imply that the materials or equipment identified are necessarily the best available for the purpose.

Acknowledgements

We acknowledge M. Gaitan and A. Jahn for their help with the confocal microscope experiments, and F. L. Degertekin and A. G. Fedorov for their hospitality and support with the ejector experiments. We also thank D. J. Ross, M. J. Fasolka, B. Hutchinson, J. Kralj, D. Reyes, S. P. Forry and W. N. Vreeland for advice and discussions. J. M. Meacham acknowledges financial support from the NIST/NRC Postdoctoral Research Program. This work was performed in part at the NIST Center for Nanoscale Science and Technology Nanofab that is partially sponsored by the NIST Office of Microelectronics Programs

References

- 1 D. Janasek, J. Franzke and A. Manz, *Nature*, 2006, **442**, 374–380.
- 2 H. Craighead, *Nature*, 2006, **442**, 387–393.
- 3 J. El-Ali, P. K. Sorger and K. F. Jensen, *Nature*, 2006, **442**, 403–411.
- 4 J. Atencia and D. J. Beebe, *Nature*, 2005, **437**, 648–655.
- 5 W. H. Wong and E. Y. B. Pun, *J. Vac. Sci. Technol., B*, 2001, **19**, 732–735.
- 6 S. Kawata and T. Tanaka, *Abstr. Pap. Am. Chem. Soc.*, 2000, **220**, U336–U336.
- 7 A. Bertsch, H. Lorenz and P. Renaud, *Sens. Actuators, A*, 1999, **73**, 14–23.
- 8 M. J. Madou, *Fundamentals of Microfabrication: The Science of Miniaturization*, CRC Press LLC, Boca Raton, FL, USA, 2002.
- 9 S. Reyntjens and R. Puers, *J. Micromech. Microeng.*, 2000, **10**, 181–188.
- 10 M. L. Kovarik and S. C. Jacobson, *Anal. Chem.*, 2006, **78**, 5214–5217.

- 11 D. J. Beebe, J. S. Moore, Q. Yu, R. H. Liu, M. L. Kraft, B. H. Jo and C. Devadoss, *Proc. Natl. Acad. Sci. U. S. A.*, 2000, **97**, 13488–13493.
- 12 W. Daschner, P. Long, R. Stein, C. Wu and S. H. Lee, *J. Vac. Sci. Technol., B*, 1996, **14**, 3730–3733.
- 13 C. M. Waits, A. Modafe and R. Ghodssi, *J. Micromech. Microeng.*, 2003, **13**, 170–177.
- 14 H. K. Wu, T. W. Odom and G. M. Whitesides, *Anal. Chem.*, 2002, **74**, 3267–3273.
- 15 C. C. Chen, D. Hirdes and A. Folch, *Proc. Natl. Acad. Sci. U. S. A.*, 2003, **100**, 1499–1504.
- 16 M. W. Toepke and P. J. A. Kenis, *J. Am. Chem. Soc.*, 2005, **127**, 7674–7675.
- 17 J. Taff, Y. Kashte, V. Spinella-Marno and M. Paranjape, *J. Vac. Sci. Technol., A*, 2006, **24**, 742–746.
- 18 J. Rauch, in *Partial differential equations and related topics*, Springer, Berlin, 1975, pp. 370–379.
- 19 J. B. Hubbard and J. F. Douglas, *Phys. Rev. E: Stat. Phys., Plasmas, Fluids, Relat. Interdiscip. Top.*, 1993, **47**, R2983–R2986.
- 20 M. L. Mansfield, J. F. Douglas and E. J. Garboczi, *Phys Rev E: Stat. Phys., Plasmas, Fluids, Relat. Interdiscip. Top.*, 2001, **64**, 061401.
- 21 H. C. Berg and E. M. Purcell, *Biophys. J.*, 1977, **20**, 193–219.
- 22 J. T. Cabral, S. D. Hudson, C. Harrison and J. F. Douglas, *Langmuir*, 2004, **20**, 10020–10029.
- 23 J. T. Cabral and J. F. Douglas, *Polymer*, 2005, **46**, 4230–4241.
- 24 G. C. Duffy, J. C. McDonald, O. J. A. Schueller and G. M. Whitesides, *Anal. Chem.*, 1998, **70**, 4974–4984.
- 25 The photolithographic contrast is the maximum slope of the plot of development rate versus exposure dose on a logarithmic scale. We calculated the contrast of our optical adhesive using data from ref. 22 Typical photoresists have a contrast of 2 to 3 (ref. 26).
- 26 S. A. Campbell, *The Science and Engineering of Microelectronic Fabrication*, Oxford University Press, New York, 1996.
- 27 We use “ppi” (pixel per inch) when we refer to the resolution of the pixelation process that we use to convert theoretical grayscale into black and white pixels, to distinguish it from the printing resolution or mask resolution that is given in “dpi” or dots per inch.
- 28 Grayscale tones close to the homogenization threshold generate surfaces with lower sidewall angle which vary depending on the pattern. Interestingly, we found that small posts ($\approx 30 \mu\text{m}$) generated with transparent pixels are vertical and form long threads, probably due to a lensing effect^{37,38}.
- 29 J. Atencia and D. J. Beebe, *Lab Chip*, 2006, **6**, 567–574.
- 30 I. Meyvantsson and D. J. Beebe, in *3rd IEEE/EMBS Special Topic Conference on Microtechnology in Medicine and Biology*, 2005, 2005, pp. 42–44.
- 31 R. H. Liu, M. A. Stremmer, K. V. Sharp, M. G. Olsen, J. G. Santiago, R. J. Adrian, H. Aref and D. J. Beebe, *J. Microelectromech. Syst.*, 2000, **9**, 190–197.
- 32 T. J. Johnson, D. Ross and L. E. Locascio, *Anal. Chem.*, 2002, **74**, 45–51.
- 33 A. D. Stroock, S. K. W. Dertinger, A. Ajdari, I. Mezic, H. A. Stone and G. M. Whitesides, *Science*, 2002, **295**, 647–651.
- 34 J. M. Meacham, C. Ejimofor, S. Kumar, F. L. Degertekin and A. G. Fedorov, *Rev. Sci. Instrum.*, 2004, **75**, 1347–1352.
- 35 A. G. Fedorov, 2007, personal communication.
- 36 The in-plane resolution is given by the size of the swatch used and by the minimum spacing required between features to avoid partial polymerization in between. Using 8×4 swatches at 2400 ppi (and 3000 dpi) the minimum patternable area size is $42 \times 84 \mu\text{m}^2$. Below 2400 ppi the optical resolution of our photolithographic set-up interferes with the fidelity of the patterns. We found empirically that the optical adhesive polymerizes forming vertical “threads” of 1 to $2 \mu\text{m}$ diameter, which sets the ultimate in-plane resolution of the fabrication process with this material if higher resolution masks are employed. Using ink masks printed at 3000 dpi and the optical adhesive, the smallest reproducible feature that we fabricated was a microchannel of constant height of $60 \mu\text{m} \pm 3 \mu\text{m}$ along the symmetry axis.
- 37 S. Shoji and S. Kawata, *Appl. Phys. Lett.*, 1999, **75**, 737–739.
- 38 A. S. Kewitsch and A. Yariv, *Appl. Phys. Lett.*, 1996, **68**, 455–457.